Bulletin of Pure and Applied Sciences
Vol.39A (Zoology), No.1,
January-June 2020: P.116-129
Original Research Article

Print version ISSN 0970 0765
Online version ISSN 2320 3188
DOI 10.5958/2320-3188.2020.00014.5
Available online at www.bpasjournals.com

One Pot Synthesis of Physico-chemically Stabilized ZnO Nanoparticles *via* Biological Method and its Potential Application as Antimicrobial Agent

[1]Manoj Singh
[2]Renu
[3]Seema Kamboj
[4]Sunil Kumari
[5]Vikas Kamboj
[6]Sushil Kumar Upadhyay*

Author's Affiliation:
[1,3,4,5,6]Department of Biotechnology, Maharishi Markandeshwar (Deemed to be University), Mullana-Ambala, Haryana 133207, India
[2]Department of Botany, S.D. (P.G.) College, Panipat, Haryana 132103, India

***Corresponding author:**
Dr. Sushil Kumar Upadhyay,
Assistant Professor, Department of Biotechnology, Maharishi Markandeshwar (Deemed to be University), Mullana-Ambala, Haryana 133207, India

E-mail:
upadhyay.k.sushil@gmail.com;
lookformanoj@gmail.com

ORCID: https://orcid.org/0000-0002-1229-4275

Received on 12.02.2020
Accepted on 25.04.2020

Abstract:
The finding was focused with an aim to synthesize stable zinc oxide nanoparticle using biomechanistic approach under optimum conditions using UV Spec, dynamic light scattering and TEM. The plant based biomolecules involved in reduction of zinc nitrate to form nanoparticles were further characterized by Fourier transform infrared analysis. Synthesis of bio-based zinc oxide nanoparticles in a physicochemical environment is an area requiring deeper investigation. The thermally stabilized nanoparticles were studied to determine the antimicrobial property. The TEM imaging confirmed that ZnO NPs were mixture of plate (spherical and hexagons) in nature and because of their inherent property of ZnO NPs bind the bacterial membrane which was confirmed through growth kinetics analysis. The carotenoids and alkaloids-functionalized metal nanoparticles suggest a potential for facilitating future research and focusing on biomedical fields.

Keywords: One pot synthesis, ZnO nanoparticle, Antimicrobial, Fourier transform infrared (FTIR), *Saraca indica,* Atomic force microscopy, Surface plasmon resonance (SPR).

INTRODUCTION

The nanoparticles are tiny particles and in terms of their transport and properties they behave as a complete unit. These smallest particles exhibit the size between 1 to 100nm. Study of nanoparticles is called nanotechnology. Nanotechnology helps in the study of physical and magnetic properties of nanoparticles. Properties of nanoparticles depend upon their size. Nanoparticles may exist in the form of suspension and colloids. The synthesis of nanoparticles can occur by using various methods including chemical and biological methods. Instead of chemical methods biological method of synthesis is more preferred due to the hazardous effect of chemicals used in the synthesis of nanoparticles. Biological synthesis of nanoparticles can be done using microbes and plants. Plants are preferred for the synthesis of nanoparticles due to the presence of various enzymes which are responsible for the reduction of metal ions to their stable form. In the process of reduction of metal ions, the biogenic reducing agents such as water soluble plant metabolites (flavonoids, terpenoids, alkaloids and phenolic compounds) and coenzymes (Murphy et al., 2004; Mukunthan and Balaji, 2012). For this purpose medicinal plants can be used for the synthesis of nanomaterials due to their medicinal properties. The aqueous extract of plants like *Saraca indica, Azadirachta indica, Catharanthus roseus* and *Ocimum sanctum* etc can be used for the synthesis of nanoparticles. Using plant extract

various nanoparticles can be synthesized such as silver, zinc oxide, gold and copper etc. (Kalluri et al., 2009; Chernousova and Epple, 2013) For the synthesis of zinc oxide nanoparticles different plants can be used including *S. indica* (ashoka tree). There are two methods of synthesis of nanoparticles such as top down and bottom up approach. Other methods of the synthesis of ZnO nanoparticles including physical and chemical methods are costly and require high temperature and non ecological chemicals (Agarwal et al., 2018). Since high energy method has resulted in toxic chemicals productions that are hazardous to environment and health, the biological method of synthesis has therefore been used. In this strategy various biological agents can be used such as plant extract, microorganism, biomolecules and ionic liquids. The aqueous extract of *S. indica* has been utilized in the synthesis of ZnO nanoparticles. The synthesized ZnO nanoparticles have been used in numerous biomedical properties due to their valuable antibacterial activities and photocatalytic activity (Ahmed et al., 2017). The natural extracts is responsible for the coating of nanoparticles with various pharmacological active molecules on zinc oxide surface which helps in the binding of nanomaterials with receptors of the bacterial membrane. These molecules may be flavonoids, aldehydes, amides, polysaccharides etc (Agarwal et al., 2018). Singh et al., (2014) reported that the main constituent of the plant extract i.e. phenol is responsible for the reduction of salt to nanostructures. The aqueous extract of *Aloe vera* is used for the synthesis of ZnO nanoparticles and is responsible for the cell damage of *Escherichia coli* due to the antibacterial activity (Ali et al., 2016). Plant extract of *S. indica* has significant antimicrobial and antibacterial activities and also act as antifungal, antidiabetic and antiulcer agent and also used against uterine disorder (Sharma et al., 2009; Muruthappan and Shree, 2010). Nanoparticles are widely used in biomedical science because of their medicinal properties. To fulfill these requirements we synthesized ZnO nanomaterials via biological method.

MATERIALS AND METHODS

Preparation of the reaction solutions:
The zinc nitrate ($Zn(NO_3)_2 \bullet 6H_2O$) was purchased from Sigma-Aldrich (Bangalore, India). The stock of the salt solution (1mM) was prepared by mixing 1.893g zinc nitrate (99.99% pure) in 100ml distilled water respectively. The water used as a solvent in this experiment was purified by double distilled water. In this study ashoka plant, *Saraca indica* (Magnoliophyta: Caesalpinaceae) leaves were collected from the campus of Maharishi Markandeshwar (Deemed to be University), Mullana-Ambala (Hryana), India and was taxonomically identified using characters and keys provided by Pradhan (2009).

Preparation of leave extract:
The freshly collected 5g plant were chopped into appropriate size (~ 1cm×1cm) and washed several times with distilled water in a 250ml conical flask. After that 100ml distilled water was added to the flask containing freshly chopped and washed plant leaves followed by the boiling at 60◦C for 15minutes. The resultant crude extract was filtered with Whatman filter paper no. 1 and stored at 4◦C and used within a week.

Synthesis and optimization of ZnO nanoparticles:
The plant filtrate was used as reducing and stabilising agent for 1mM $Zn(NO_3)_2 \bullet 6H_2O$. In a typical synthesis of zinc oxide (ZnO) nanoparticles for the reduction of Zn^{2+} ions, the 5ml filtrate was added to 30ml of 10^{-3}M $ZnNO_3$ solution in a 250ml flask and kept on a rotary shaker (120rpm) at 30◦C (Canizal et al., 2006; Farooqui et al., 2010; Nagati et al., 2012). The effects of different parameters were studied to obtain optimum maximum synthesis of ZnO nanoparticles and particle size distribution. The nanoparticles synthesis was optimized by varying the different parameters at a time after Willander et al. (2009) and Pachauri et al. (2010). The different parameters selected were mixing ratio (1:6, 1:7, 1:8 and 1:9), reaction temperature (50◦C, 60◦C, 70◦C and 80◦C and reaction time (0hr, 1hr, 2hrs, 4hrs, 5hrs, 6hrs and 24hrs).

Purification and characterization of zinc oxide nanoparticles:
An optimal centrifugation process was obtained based at 10,000rpm for 10minutes to remove the non-ZnO nanoparticles along with a maximal recovery from the synthesized solution. The supernatant was collected and frozen at −70◦C for 45minutes for 2 days using lyophillizer (Micro Modulyo 230

freeze dryer, Thermo Electron Corp., India). The lyophilized nanoparticles were stored desiccated at 4°C. The characterization of zinc oxide nanoparticles (ZnO NPs) was performed using different techniques including UV-visible spectrophotometer (UV-Vis) can be utilized to study the unique optical properties of nanoparticles (Haiss et al., 2007). The UV-Vis spectroscopy measurements were recorded on a Shimadzu dual-beam spectrophotometer (model UV 2500, Japan) operated at a resolution of 1nm between 300 and 700nm in a 10mm path length quartz cuvette. The Dynamic Light Scattering (DLS), the medium size, distribution and the zeta potential of the prepared ZnO NPs were analyzed by photon correlation spectroscopy using a zeta sizer PALS (Phase Analysis Light Scattering) zeta potential analyzer ver. 3.54 (NCL, Pune). Atomic Force Microscopy (AFM, APE research: AI00SGS; USA) was performed to examine the 3D–structures of nanoparticles to analyze the topography and size of the engineered nanoparticles (Magonov et al., 1997). The Transmission Electron Microscopy (TEM) was used for high resolution imaging of thin films of a solid sample for ZnO nanostructure and compositional analysis. The topographic information obtained by TEM in the vicinity of atomic resolution utilized for structural characterization and identification of various phases of nanomaterials, *viz*., hexagonal, cubic or lamellar (Akhbari et al., 2016). The Fourier Transformed Infrared (FTIR) spectroscopy deals with the vibration of chemical bonds in a molecule at various frequencies depending on the elements and types of bonds (Dubey et al., 2010). The FTIR was done to examine surface characterization of various chemical and conformational changes of nanoparticles samples.

***In vitro* bacterial growth kinetics analysis:**

The formulated ashoka oil nanoemulsion was selected to study the minimum inhibitory concentration (MIC) on bacterial growth inhibition (Abbas et al., 2013). The grown bacterial inoculum of *E. coli* was centrifuged at 5000rpm for 10minutes. The pellet obtained was washed with phosphate buffer saline (PBS). The process of redispersion in sterile phosphate buffer saline was repeated after every centrifugation to obtain better separation of pellet from entities. The optical density of bacterial inoculum was adjusted to 10^{-8}CFU/ml using phosphate buffer saline at 400nm. The 0.1ml of the freshly prepared bacterial inoculum was added in sterile side arm Erlenmeyer flask (250ml) containing 50ml nutrient broth. The 1ml of different concentrations (1µg/ml, 2µg/ml, 3µg/ml, 5µg/ml and 7µg/ml) of optimized ashoka oil nanoemulsion was added to the nutrient broth. The uniform mixing of bacterial broth and nanoemulsion to minimize aggregation was achieved upon incubation on rotary orbital shaker at 200rpm and 28-30°C. The experiment was conducted by including positive control (flask containing ashoka oil nanoemulsion and nutrient broth) and negative control (flask containing bacterial inoculum and nutrient media) after Holstrom et al. (2003). The growth kinetics rate was monitored at regular time interval by measuring the optical density at 450nm for ZnO and the experiment was carried out in triplicate to avoid standard error.

RESULTS

During investigation 1mM zinc nitrate salt solution was used as reducing agent with 5% plant leaf extract at room temperature in the ratio of 1:8 (*v/v* mixing ratio) for the biosynthesis of ZnO NPs (zinc oxide nanoparticles). The Zn^{2+} ions were reduced into ZnO NPs and were characterized by using modern reliable tools and techniques. The formation of zinc oxide nanoparticles was primarily observed with the change in color from yellow to creamish solution. The intensity of light creamish coloration was directly proportional to the incubation period and reduction of zinc nitrate.

Characterization of ZnO NPs using UV-Vis spectroscopy:

The light absorption pattern of the plant biomass was kinetically monitored with the help of UV-Vis measurement at particular time interval (Fig. 1). The spectra showed a well-defined surface plasmon band for ashoka plant between 400-450nm, which was the characteristic of ZnO nanoparticles and clearly indicates the formation of nanoparticles in solution. The spectrophotometric analysis of the colloidal zinc showed the moderate stability with turbid appearance at both the reaction peaks (i.e. 400nm and 450nm). It was also observed that the maximum absorbance occurs at 450nm and steadily increase in intensity as a function of reaction time. The initial absorption intensities at 350nm for ZnO nanoparticles were near to 2a.u, the different peaks for absorbance was monitored with increase in time duration. The maximum absorbance was found to be 3.08a.u after 5hrs of synthesis. The zinc

oxide nanoparticles solution was found to be extremely stable for *S. indica* with little evidence of flocculation of the particles even a month after the reaction. The resonance was sharp and indicated little aggregation of zinc oxide nanoparticles in solution. The surface plasmon resonance (SPR) bands were little broad with an absorption tail in the longer wavelength region for ashoka plants.

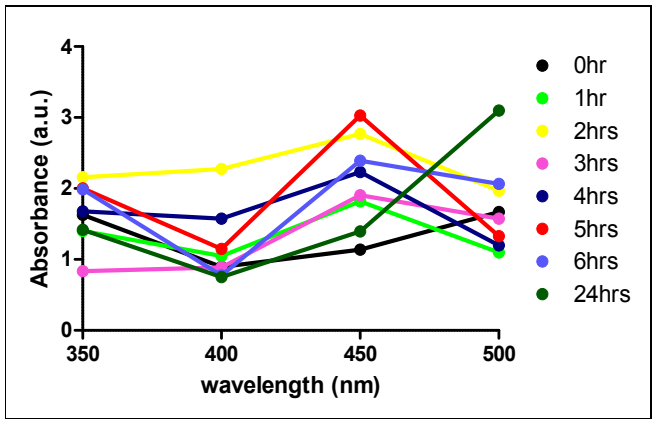

Figure 1: UV-Vis spectra recorded with respect to time after the reaction of 1mM Zinc nitrate solution with 5% *S. indica* aqueous leaf extract for 24hrs.

Characterization of ZnO NPs using atomic force microscopy

The crude nanoparticle extract of the plant was analysed for size distribution as a part of screening through AFM. The AFM was performed on the glass substrate in tapping mode, for the reaction mixture of 24hrs incubation periods. The obtained morphology revealed the fact that the synthesized zinc oxide nanoparticles were polydispersed and polyshaped. The two and three-dimensional study of bio-functionalized ZnO NPs was done by AFM to study the topographical view and size pattern of nanoparticles. The AFM images of the bio-functionalized organic layer which consists of rich concentration of organic moieties at the surface confirmed the polydispersity of the nanoparticles. The particle size in the AFM image of zinc oxide nanoparticles synthesized by *S. indica* was ~0-66nm showed heterogeneous vertical and lateral dimensions since stacking defaults of zinc poly shaped nanotriangles (Fig. 2). The three-dimensional images of these nanostructures showed little surface roughness.

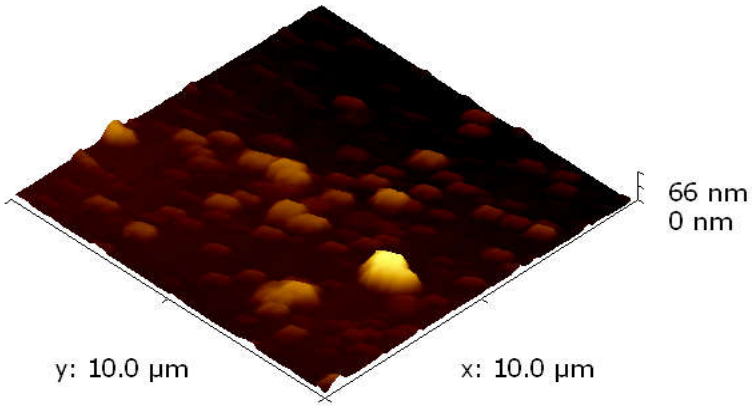

Figure 2: AFM image of zinc oxide nanoparticles synthesized by *S. indica.*

Optimization of physico–chemical parameters

The surface plasmon resonance (SPR) spectra for ZnO NPs synthesized from leaf extract of *S. indica* were obtained at 450nm. The change in colour from yellow to cream confirmed the synthesis of zinc oxide nanoparticles (Fig. 3). The wavelength spectrum (lambda maximum) for all considered parameters was constant during the reaction process.

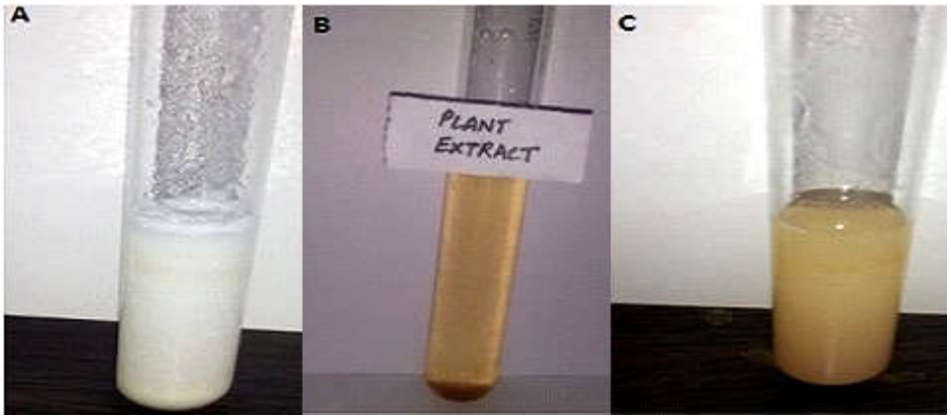

Figure 3: The spectral signature of ZnO NPs. Milky white ZnO salt solution (A), Yellow aqueous leaf extract of *S. indica* (B), Creamish color indicating the formation of ZnO NPs (C).

Effect of mixing ratio

The effect of different mixing ratio concentration for rapid biological synthesis of zinc oxide nanoparticles from 5% *S. indica* leaf broth was studied in terms of intensity. The absorbance was measured at different time intervals. At different mixing ratio concentration the sharpness in the absorbance intensity of the plasmon peak changed rapidly by varying mixing ratio concentration (1:6, 1:7, 1:8 and 1:9) of 1mM (Figs. 4-7). The maximum absorbance was achieved with 1:8 mixing ratio concentration of Zn ion.

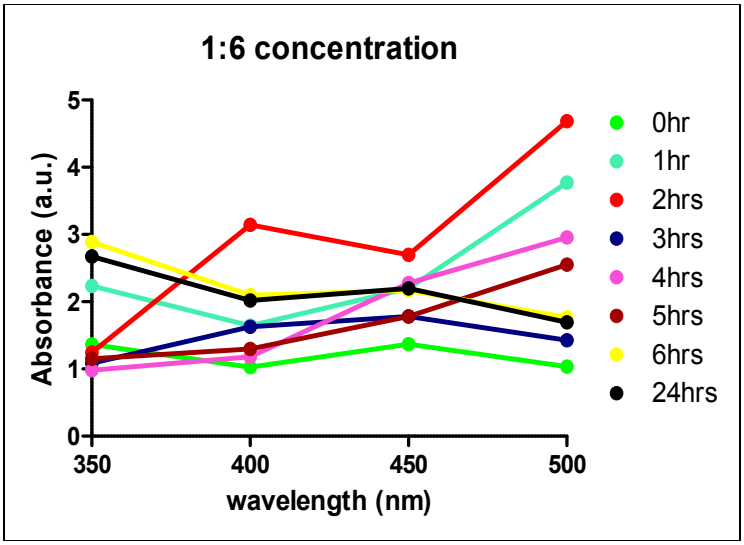

Figure 4: The effect of metal ion on SPR of ZnO NPs with 1:6 mixing ratio.

The initial absorption intensities at 350nm for zinc oxide nanoparticles were 1.24a.u, the different peaks for absorbance was monitored with increase in time duration. The maximum absorbance was found to be 3.14a.u after 2hrs of synthesis.

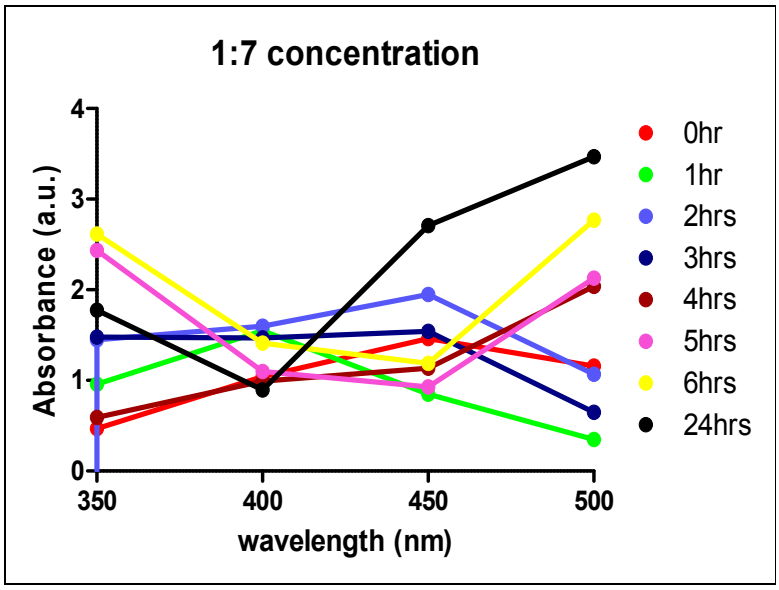

Figure 5: The effect of metal ion on SPR of ZnO NPs with 1:7 mixing ratio.

The initial absorption intensities at 350nm for zinc oxide nanoparticles were 1.44a.u, the different peaks for absorbance was monitored with increase in time duration. The maximum absorbance was found to be 1.98a.u after 2hrs of synthesis.

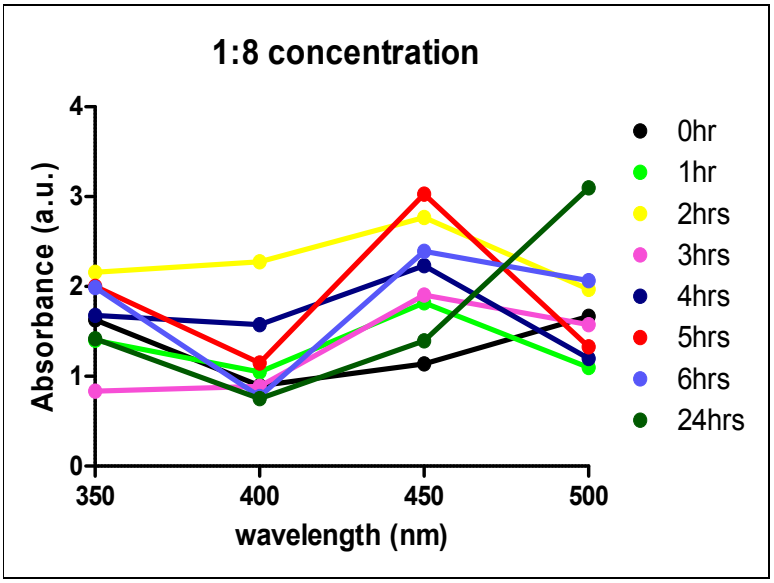

Figure 6: The effect of metal ion on SPR of ZnO NPs with 1:8 mixing ratio.

The initial absorption intensities at 350nm for zinc oxide nanoparticles were near to 2a.u, the different peaks for absorbance was monitored with increase in time duration. The maximum absorbance was found to be 3.02a.u after 5hrs of synthesis at 450nm.

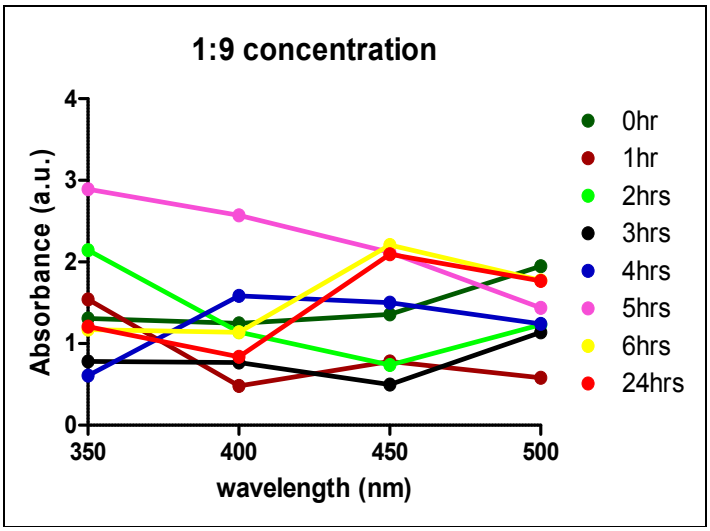

Figure 7: The effect of metal ion on SPR of ZnO NPs with 1:9 mixing ratio.

The initial absorption intensities at 350nm for zinc oxide nanoparticles were 1.17a.u, the different peaks for absorbance was monitored with increase in time duration. The maximum absorbance was found to be 2.20a.u after 6hrs of synthesis.

Effect of reaction temperature

The absorbance was taken after heating of the sample at different temperature showed variable rate of synthesis at different mixing ratio for zinc oxide nanoparticles using 5% *S. indica* leaf broth (Fig. 8). The finding showed that after heating of 1:6 mixing ratio at 50°C, the initial absorption intensities were 1.46a.u but there is a slight decrease in the synthesis of nanoparticles when the sample was heated at 60°C and is reduced to 1.31a.u on the other hand slightly increased after heating at 80°C. In the case of 1:8 mixing ratio, when the sample was heated at 50°C, the synthesis of nanoparticles was slow with 3.48a.u but when the sample was heated at 60°C the absorption intensity was decreased to 1.38a.u, however, increased after heating at 80°C temperature. The other mixing ratio i.e. 1:7 and 1:9 were showed similar pattern of synthesis with the increasing temperature but 1:9 mixing ratio showed a slight increase in absorption intensity at 70°C temperature. The zinc oxide nanoparticles synthesis rate increased proportionately to the reaction temperature. At room temperature, there was an initial lag period for the formation of zinc nuclei and the rate of synthesis was slow. The maximum absorbance intensity was achieved at 60°C indicated the higher conversion of zinc ions into zinc oxide nanoparticles. The rate of reduction to zinc nanoparticles was almost faster at all reaction temperatures.

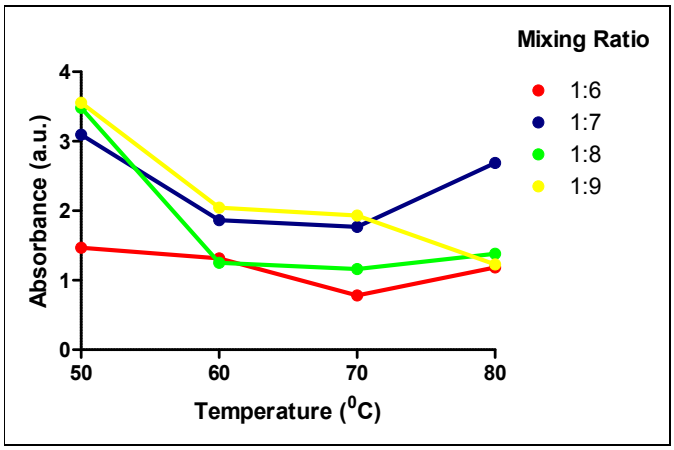

Figure 8: The effect of temperature on SPR of ZnO NPs with different mixing ratio.

Effect of reaction time:

The finding showed the different absorbance value recorded at 450nm from the aqueous solution of 1mM $ZnNO_3$ as a function of reaction time using *S. indica* leaf extract at 60°C (Fig. 9). The study showed that after heating of 1:6 mixing ratio at 60°C synthesis of nanoparticles started and increased to 3.14a.u.after 2hrs of synthesis followed some random synthesis and became stable. In 1:8 mixing ratio, when sample was heated at 60°C temperature the synthesis of nanoparticles started which rose to 2.27a.u after 2hr of synthesis and then the synthesis became stable. The other mixing ratio i.e. 1:7 showed poor synthesis, however, 1:9 ratios reflected random pattern of synthesis in initial period while after 5hrs of synthesis the absorption intensity increased to 2.57a.u and then became stable. Thus mixing ratio 1:6 showed maximum absorption about 3.14a.u after 2hrs of synthesis. The formation of zinc oxide nanoparticles started within 1hr of the reaction and absorbance were recorded at regular interval. The rate of absorbance increased with increase in time but after 24hrs, there was no further change in the absorption intensity.

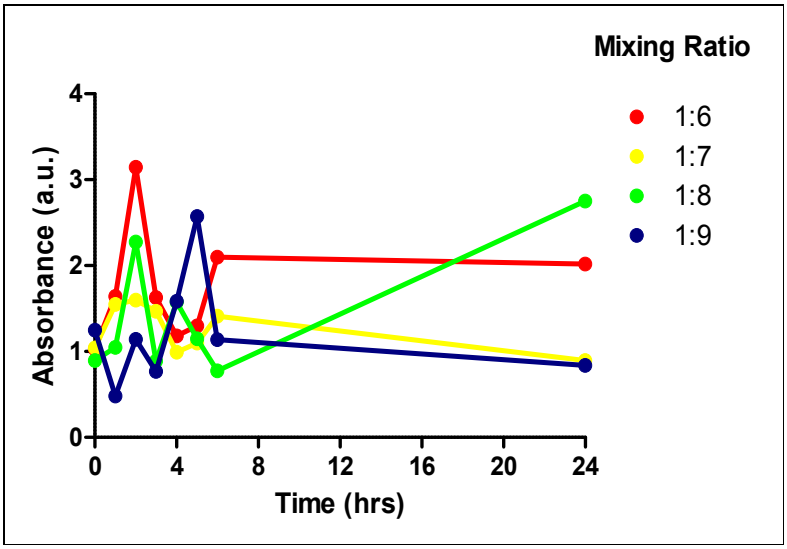

Figure 9: The effects of incubation time on SPR of ZnO NPs with different mixing ratio.

Purification and lyophilisation of ZnO NPs

The non-ZnO NPs components were removed along with a maximal recovery of ZnO NPs colloids from the synthesized solution at variable optimal centrifugation forces. Therefore freeze-drying process of zinc oxide nanoparticles (nanoparticles suspensions) was performed in order to improve their physico-chemical stability.

Physico-chemical properties of ZnO NPs

Particle size distribution and zeta potential of ZnO NPs: The biofunctionalized zinc oxide nanoparticles synthesized from the aqueous solution of 1mM $ZnNO_3$ using 5% aqueous leaves extract of *S. indica* at 60°C temperature was characterized for particle size distribution determined by the DLS technique (Fig. 10). The peak number and peak amplitude obtained gave important explanation for size and size distribution of zinc oxide nanoparticles. There was double peak at Zeta Sizer distribution, confirmed the narrow distribution of zinc oxide nanoparticles. There was single peak at Zeta Sizer distribution, confirmed the narrow distribution of zinc oxide nanoparticles. The calculated particle size distribution by intensity was observed in the range of 50–110nm (Fig. 10). It can be seen that the mean particle size was 59.81nm with some particles having diameters above 1000nm. The polydispersity index (pdI) was noticed 0.353.

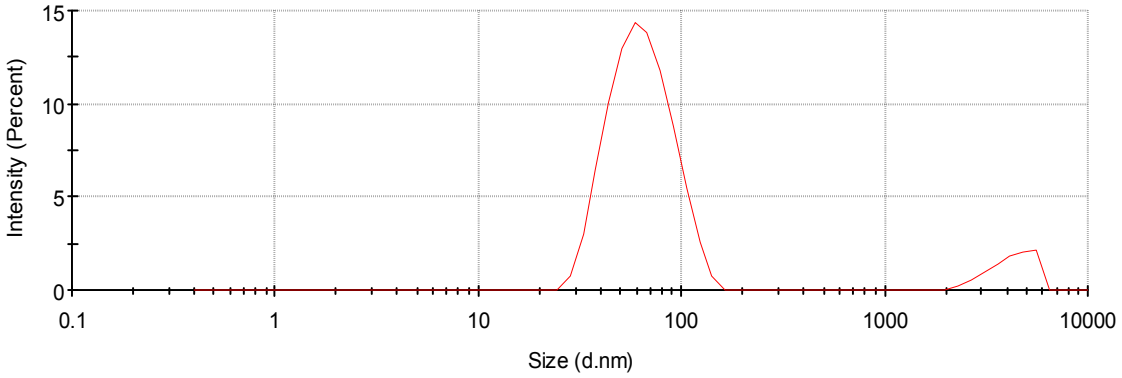

Figure 10: DLS size distribution of ZnO NPs obtained from reduction of 1mM $ZnNO_3$ at 60°C.

Atomic force microscopy of ZnO NPs: Zinc oxide nanoparticles was conducted. The topography image explained the polydispersed zinc oxide nanoparticles at 60°C with maximum size of 0-52.4nm (Fig. 11). The sample surface was non-agglomerated and polydispersed as confirmed by two- and three-dimensional view of distribution. The AFM measurements were made using the tapping mode developed especially for studying bio-functionalized samples. The AFM image of one of the regions consists of rich concentration of organic moieties at the surface.

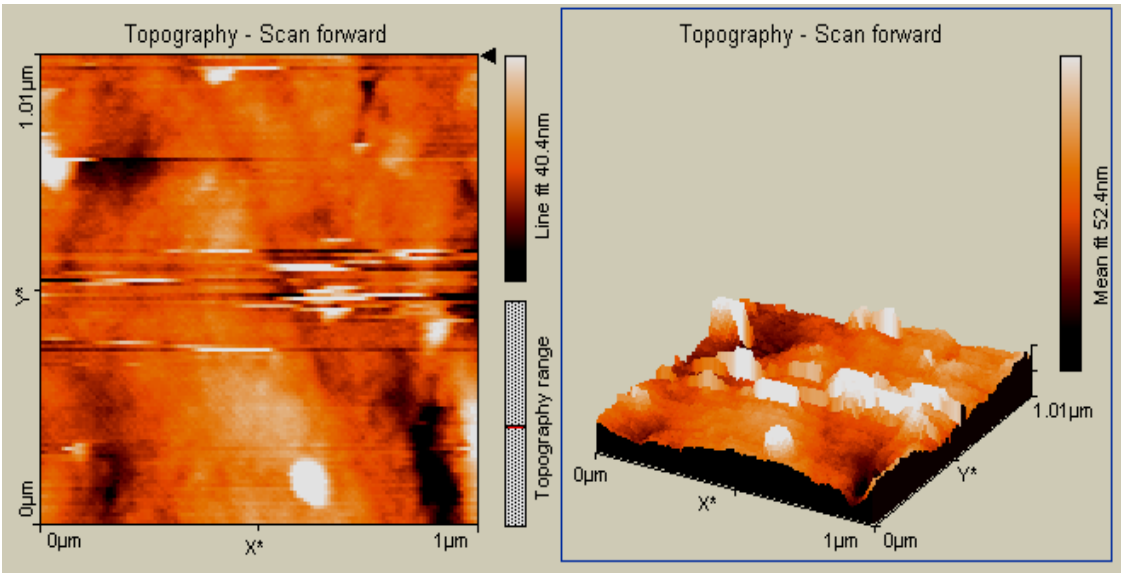

Figure 11: AFM image of zinc oxide nanoparticles synthesized at 60°C from reaction mixture of 5% aqueous leaves extract of by *S. indica* and 1mM $ZnNO_3$ solution.

Transmission electron microscopy: The zinc oxide nanoparticles fabricated using 5% *S. indica* leaf broth and 1mM $ZnNO_3$ solution at 60°C monitored for shape and size distribution of nanoparticles. A mixture of plate (spherical and hexagons) and spheres were obtained in large number at 60°C (Fig. 12). Representative transmission electron microscopy (TEM) images and corresponding size distribution histogram of ZnO NPs were ranging from 50 to 100nm. The high-resolution TEM (HR-TEM) images displayed clear lattice fringes on the particle surfaces.

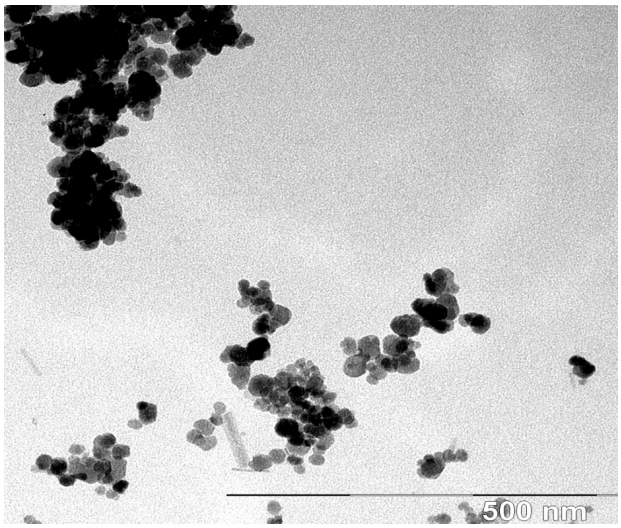

Figure 12: TEM micrograph of a drop-coated film of ZnO aqueous solution formed by 1mM $ZnNO_3$ and 5% *S. indica* leaf broth at 60°C.

Fourier transform infra-red (FTIR) spectroscopy: The FTIR analysis was used for the functional group characterization from the *S. indica* leaves extract and synthesized zinc oxide nanoparticles at 60°C (Fig. 13). The absorbance bands were observed in the region of 500–4500cm^{-1}. The ZnO NPs synthesized at 60°C showed stronger intense peak at 3421cm^{-1}, 2118cm^{-1} and 1654cm^{-1} (Fig. 13). The maximum intense peak 3421 cm^{-1} corresponds to stretching mode of vibration of amine group. The intense peak 2118cm^{-1} corresponds to stretching mode of vibration of alkyne group and the intense peak on 1654cm^{-1} correspond to alkene group. The other formed peaks like 1314cm^{-1}, 1402cm^{-1}, 1416cm^{-1} corresponded to methyl functional group, however 952cm^{-1} to C-F (carbonyl falvonoids) group.

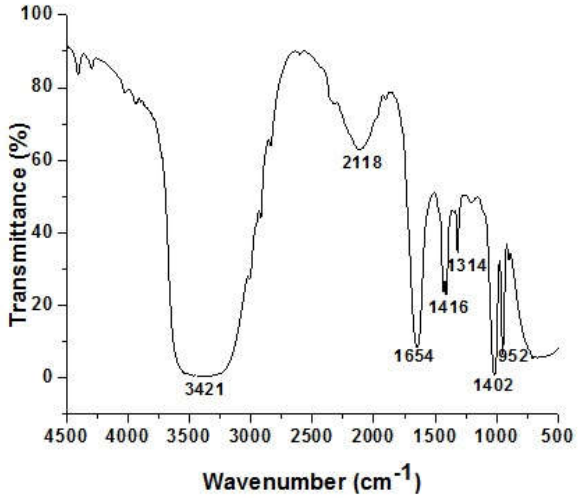

Figure 13: The FTIR spectra of zinc oxide nanoparticles (ZnO NPs).

Growth curve analysis of bacterial cells

The growth curve of *E. coli* treated with biologically synthesized ZnO NPs, plant extract and zinc nitrate as positive and negative control (Fig. 14). The concentration of 5µg/ml and 7µg/ml showed poor growth of *E. coli* which was comparatively lesser than with the growth seen at lower concentration. It was very interesting to observe that the incorporation of 7µg/ml ZnO NPs to nutrient broth showed maximum inhibition of *E. coli* in comparison to plant extract solution (Fig. 14A,

C). It was also noticed that $ZnNO_3$ salt solution was also able to inhibit the growth of *E. coli* (Fig. 14B). The dynamics of bacterial growth was monitored with broth supplement with 10^{-8} *E. coli* cells using 3µg/ml, 5µg/ml and 7µg/ml of ZnO NPs at all these concentration reflected delayed growth of *E. coli*. The growth kinetics of *E. coli* bacteria was monitored continuously for 24hrs of their incubation under different concentration of ZnO NPs, $ZnNO_3$ solution and plant extract (Fig 14). The lowest concentration of $ZnNO_3$ (1µg/ml) also had effect on bacterial growth whereas at the same concentration ZnO NPs and plant extract had no effect in bacterial growth. Higher concentration caused a growth delay or inhibition for $ZnNO_3$ in comparison to other samples. Thus Kinetic analysis suggested that growth of *E. coli* bacteria was affected even by low concentration of $ZnNO_3$ solution in comparison to ZnO NPs and plant extract solution. The $ZnNO_3$ solution also showed antibacterial activity on higher concentration after 12hrs of incubation whereas the plant extract showed antibacterial activity at higher concentration after 20hrs of incubation.

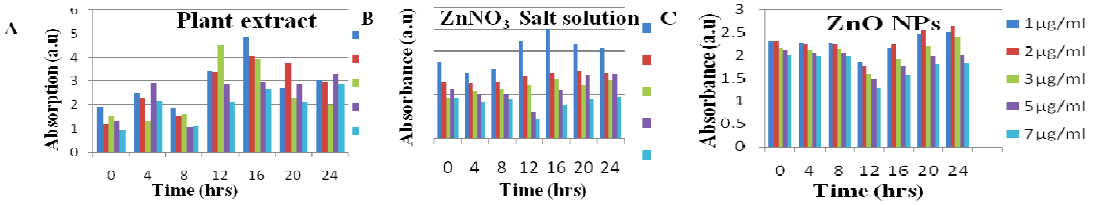

Figure 14: Antibacterial activity showed by aqueous extract of *S. indica* (A), Zinc nitrate salt solution (B), and Zinc oxide nanoparticles (C).

DISCUSSION

The process to development of reliable and eco-friendly metallic nanoparticles is an important step in the field of nanotechnology. It can be achieved by the use of natural resources like biological systems are most essential objects. In recent years, zinc oxide nanoparticles have been widely used in diverse biomedical applications because of their efficient optical and electronic properties. This metal nanoparticle poses a strong surface chemistry which renders them suitable for attachment with biomolecules (Mukunthan and Balaji, 2012; Ahmed et al., 2017). This research focused on biological synthesis of metallic nanoparticles for biomedical application. A variety of chemical and physical procedures has been used for synthesis of metallic nanoparticles (Kalluri et al., 2009; Chernousova and Epple, 2013; Ali et al., 2016; Agarwal et al., 2018). However, these methods were fraught with many problems including use of toxic solvents, generation of hazardous by-products, and high energy consumption. Accordingly, there was an essential need to develop environmentally benign procedures for synthesis of metallic nanoparticles. A promising approach to achieve this objective was to exploit the array of biological resources in nature (Chakraborty et al., 2018). Over the past several decades, Green synthesis of nanoparticle depends on plant source and the organic compound in the crude leaf extract (Sharma et al., 2009). It had no harmful particles to help in building better products. In the midst of the assorted biosynthetic approaches the use of plant extracts was ease of availability, safe to handle and cost effective. An economic novel alternative choice for chemical and physical methods of nanoparticles synthesis was green method (Reed and Hutchison, 2000). The ZnO NPs synthesized using ashoka plant showed their characteristic peaks at 450nm respectively, which is the confirmatory feature for zinc oxide nanoparticles formation due to the excitation of surface plasmon vibrations in metal nanoparticles (Bhumkar et al., 2007). Our findings were also supported by Singh et al. (2012) who reported that polyshaped nanoparticles absorb the wavelength in the NIR region of the electromagnetic spectrum, which corresponds to the longitudinal surface plasmon absorption.

During the present investigation the formation of metal nanoparticles were obtained at medium salt concentration (1mM). This finding was supported by Ogale et al. (2006), who made a conclusion that 1mM gold concentration produced good absorbance resulted in narrow particle size distribution curve. The other important variable was the effect of reaction temperature. In the present workout, it was also observed that the rate of reaction increased the absorbance with increase in reaction

temperature in very short duration. The size distribution was further confirmed by TEM. The rate of synthesis got reduced after an optimum temperature thus maximum absorbance obtained at λ_{max} was at 60°C for zinc oxide nanoparticles. The change in the absorbance with the reaction temperature was corroborated to the findings of Song et al. (2009).

The other important variable was the effect of mixing concentration of salt and plant extract solution. It was observed that the maximum rate of synthesis was at 1:8 mixing ratio for zinc oxide nanoparticles synthesis. This was further supported and validated by TEM analyses which concluded that nanoparticles were polydispersed in the range of 50-100nm for ZnO NPs. The changes in the absorbance with the different mixing ratio for metal nanoparticle synthesis were supported by Singh et al. (2012). The results as noted in DLS images were high agreeable to the observations made under AFM results (Robert et al., 2003). Large plate structures could not be detected and most particles were hexagonal or spherical similar to the findings reported by Song et al. (2009) who made control over the shape and size of metallic nanoparticles. The probable pathway of biosynthesis was studied using FTIR spectroscopy. Therefore the synthesized nanoparticles were surrounded by metabolites such as terpenoids having functional group of carbonyl, flavonoids and steroid was confirmed (Govindachari et al., 1992). Different biological compounds such as flavonoids, lignin glycosides, lyoniside, tannins, quercetin, alkaloids, alcohol and beta-sitosterol from leaves formed a strong capping on the nanoparticles (Perkins, 1986; Perkins, 1987).

The variation in concentration of ZnO NPs was effective in *vitro* against the tested bacterial species. The overall antibacterial efficacy of ZnO NPs, $ZnNO_3$ and plant extract developed against *E. coli* (Cavassin et al., 2015). Zhou and Tang (2018) also reported that a concentration of 10µg/ml of ZnO NPs showed strong antibacterial activity against *E. coli*. Most of the factors noted to modify the antibacterial effect of ZnO NPs were size, shape, stability and concentration (Sirelkhatim et al., 2015). The size dependent activity of ZnO NPs attributed to a relative increase of surface area to volume ratio of NPs. The larger size of NPs showed similar results to that of smaller size NPs. The agglomeration was more evident after co-incubation of ZnO NPs with the pathogens, due to the additional binding of nanoparticles to cell debris. Since nanoparticles were known to absorb biomolecules and agglomerate in the biological mediums that was usually tested (Singh et al., 2014). The efficacy of these variables might be different in dry surfaces, which could be the subject of another study.

CONCLUSIONS

It is predicted that nanotechnology will have a $3.1 trillion impact on the global economy by 2020. The projected nanotechnology market is expected to be about US$25 billion in 2012. Seeing the increasing demand of these highly unpredictable and amoebic types of gold nanoparticles and best possible medical application, we have successfully biosynthesized the zinc oxide nanoparticle using ashoka plant (*Saraca indica*) leaves. The green synthesis of zinc oxide nanoparticles (ZnO NPs) using leaf extract of *S. indica* has potential to act as antibacterial agent against both gram-positive and gram-negative strains. Overall results obtained during this work have shown that the metal nanoparticles have promising results in growth kinetics against gram negative bacteria. This exploration creates the new avenue to a new standard where the different carotenoids and alkaloids-functionalized metal nanoparticles can be a powerful contrivance in the field of nanomedecine. Thus, the development of biosynthetic approaches and bio-functionalized targeted metal nanoparticles as therapeutic agents will generate great interest in both academy and industry for mankind and economy.

ACKNOWLEDGEMENTS

Authors are sincerely grateful to the authorities of Maharishi Markandeshwar (Deemed to be University), Mullana-Ambala, Haryana, India for invariable prop up during experimentation and assemblage of findings.

REFERENCES

1. Abbas S, Hayat K., Karangwa E, Bashari M, Zhang X (2013) An Overview of Ultrasound-Assisted Food-Grade Nanoemulsions. Food Eng Rev 5(3): 139–157.
2. Agarwal H, Menon S, Kumar SV and Rajeskumar S (2018) Mechanistic study on antibacterial action of Zinc oxide nanoparticles synthesized using green route. Chem Biol Inter 286: 60–70.
3. Ahmed S, Annu, Chaudhary SA and Ikram S (2017) A review on biogenic synthesis of ZnO nanoparticles using plant extract and microbes: A prospect towards green chemistry. J Photochem Photobiol (Biol) 166: 272–284.
4. Ali K, Dwivedi S, Azam A, Saquib Q, Al-said M.S, Alkhedhairy A.A (2016). Aloe vera extract functionalized zinc oxide nanoparticles as nanoantibiotics against multi-drug resistant clinical bacterial isolates. J. Colloid Interface Sci, 472 :145-156.
5. Bhumkar DR, Joshi HM, Sastry M and Pokharkar VB (2007) Chitosan reduced gold nanoparticles as novel carriers for transmucosal delivery of insulin. Pharma Res 24: 1415–1426.
6. Canizal G, Schabes-Retchkiman PS, Pal U, Liu HB and Ascencio AJ (2006) Controlled synthesis of ZnO nanoparticles by bioreduction. Mater Chem Phys 97: 321–329.
7. Cavassin ED, de Figueiredo LF, Otoch JP, Seckle MM, de Oliveira RA, Franco FF, Marangoni VS, Zucolotto V, Levin AS and Costa SF (2015) Comparison of methods to detect the *in vitro* activity of silver nanoparticles (Ag NP) against multidrug resistant bacteria. J Nanobiotech 13: 64p.
8. Chernousova S and Epple M (2013) Silver as antibacterial agent: Ion, nanoparticle, and metal. Angew Chem Int Ed Engl 52: 1636–1653.
9. Dubey SP, Lahtinen M and Sillanpaa M (2010) Green synthesis and characterization of silver and gold nanoparticles using leaf extract of *Rosa rugosa*. Colloids Surf Physicochem Eng Asp 364: 34–41.
10. Farooqui MDA, Chauhan PS, Krishnamoorthy P and Shaik J (2010) Extraction of silver nanoparticles from the leaf extracts of *Clerodendrum inerme*. Dig J Nanomater Biostruct 5(1): 43–49.
11. Govindachari T, Sandhya G and Ganesh SR (1992) Simple method for the isolation of azadirachtin by preparative high performance liquid chromatography. J Chromatogr 513: 389–391.
12. Haiss W, Nguyen TK, Aveyard J and David G (2007) Determination of size and concentration of gold nanoparticles from UV-Vis spectra. Analyt Chem 79: 4215–4221.
13. Holstrom K, Graslund S, Wahlstrom A, Poungshompoo S, Bengt-Erik B, and Kautsky N (2003) Antibiotic use in shrimp farming and implications for environmental impacts and human health. I J Food Sci Tech 38, 255–266.
14. Kalluri JR, Tahir A, Khan SA, Neely A, Candice P, Varisli B, Washington M, McAfee S, Robinson B, Banerjee S, Singh AK, Senapati S and Ray PC (2009). Use of gold nanoparticles in a simple colorimetric and ultrasensitive dynamic light scattering assay: Selective detection of Arsenic in groundwater. Angew Chem Int Ed 48: 1–5.
15. Magonov SN and Reneker DH (1997) Characterization of polymer surfaces with atomic force microscopy. Ann Rev Mater Res 27: 175–222.
16. Mirzadeh E and Akhbari K (2016) Synthesis of nanomaterials with desirable morphologies from metal-organic frameworks for various applications. Cryst Eng Comm 18: 7410–7424.
17. Mukunthan KS and Balaji S (2012) Cashew apple juice (*Anacardium occidentale* L.) speeds up the synthesis of silver nanoparticles. Int J Grn Nanotech 4: 71–79.
18. Murphy D, Redmond G, De La Torre BG and Eritja R (2004) Hybridization and melting behavior of peptide nucleic acid (PNA) oligonucleotide chimeras conjugated to gold nanoparticles. Helva Chim Acta 87(11): 2727– 2734.
19. Muruthappan V and Shree SK (2010) Anti-ulcer activity of aqueous suspension of *Saraca indica* flower against gastric ulcer in albino rats. J Pharma Res 3(1): 17–20.

20. Nagati V, Koyyati R, Donda MR, Alwala J, Kundle KR and Padigya PRM (2012) Green synthesis and characterization of Silver nanoparticles from Cajanus cajan leaf extract and its antibacterial activity. Int J Nanometer Biostruct 2: 39–43.
21. Ogale SB, Ahmad A, Pasricha R, Dhas VV and Syed A (2006) Physical manipulation of biological and chemical synthesis for nanoparticle shape and size control. *Appl Phys Lett* 89(26): 263105–263108.
22. Pachauri V, Vlandas A, Kern K and Balasubramanian K (2010) Site-specific self-assembled liquid-gated ZnO nanowire transistors for sensing applications. Small 6(4): 589–594.
23. Perkins WD (1986) Fourier Transform- Infrared Spectroscopy. Part 1: Instrumentation. J Chem Educ pp 63.
24. Perkins WD (1987) Fourier Transform- Infrared Spectroscopy. Part 2: Advantages of FT-IR. J Chem Educ pp 64.
25. Pradhan P, Joseph L, Gupta V, Chulet R, Arya H, Verma R and Bajpai A (2009) A review on ashoka. J Chem Pharma Res 1(1): 62–71.
26. Reed SM and Hutchison JE (2000) Green chemistry in the organic teaching laboratory: An environmentally benign synthesis of adipic acids. J Chem Educ 77: 1627–1628.
27. Robert, BB, David JB, Toca-Herrera LJ, Blake AW, Smith DA and Radford SE (2003). Force mode atomic force microscopy as a tool for protein folding studies. Analyt Chim Acta 479(1): 87–105.
28. Sharma VK, Yngard RA and Lin Y (2009) Silver nanoparticles: Green synthesis and their antibacterial activities. Adv Colloid Inter Sci 145(1-2): 83–96.
29. Singh M, Kumar M, Manikandan S, Chandrasekaran N, Mukherjee A, et al. (2014) Drug Delivery System for Controlled Cancer Therapy Using Physico-Chemically Stabilized Bioconjugated Gold Nanoparticles Synthesized from Marine Macroalgae, Padina Gymnospora. J Nanomed Nanotechol S5:009. doi:10.4172/2157-7439.S5-009.
30. Singh M, Chandrasekaran N, Mukherjee A et al (2014) Cancerous cell targeting and destruction using pH stabilized amperometric bioconjugated gold nanoparticles from marine macroalgae, *Padina gymnospora*. Bioprocess Biosyst Eng 37:1859–1869.
31. Singh M, Kalaivani R, Manikandan S, Sangeetha N and Kumaraguru AK (2012) Facile green synthesis of variable metallic gold nanoparticle using *Padina gymnospora*, a brown marine macroalga. Appl Nanosci 2(8): 1–7.
32. Sirelkhatim A, Mahmud S, Seeni A, Kaus NHM, Ann C, Bakhori SKM (2015) Review on zinc oxide nanoparticles: antibacterial activity and toxicity mechanism. Nano-Micro Lett, 7:219-242.
33. Song JY, Jang HK and Kim BS (2009) Biological synthesis of gold nanoparticles using *Magnolia kobus* and *Diopyros kaki* leaf extracts. Process Biochem 44: 1133–1138.
34. Willander M and Al-Hilli SM (2009) ZnO nanorods as an intracellular sensor for pH measurements. Micro Nano Techn Bioanal 102: 187–200.
35. Zhou Y and Tang RC (2018) Facile and eco-friendly fabrication of Ag NPs coated silk for antibacterial and antioxidant textiles using honeysuckle extracts. J Photochem Photobiol 178: 463–471.